Investigation on Localized States in GaN Nanowires

L. Polenta,[†,*] M. Rossi,[†] A. Cavallini,[†] R. Calarco,[‡] M. Marso,[‡] R. Meijers,[‡] T. Richter,[‡] T. Stoica,[‡] and H. Lüth[‡]

[†]CNISM and Physics Department, University of Bologna, V.le Berti-Pichat 6/2, 40127 Bologna, Italy, and [‡]Institute of Bio- and Nanosystems (IBN1) and cni—Center of Nanoelectronic Systems for Information Technology, Research Centre Jülich, 52425 Jülich, Germany

ABSTRACT GaN nanowires with diameters ranging between 50 and 500 nm were investigated by electrical and photoinduced current techniques to determine the influence of their size on the opto-electronic behavior of nanodevices. The conductivity, photoconductivity, and persistent photoconductivity behavior of GaN nanowires are observed to strongly depend on the wire diameter. In particular, by spectral photoconductivity measurements, three main sub-band-gap optoelectronic transitions were detected, ascribed to the localized states giving rise to the characteristic blue, green, and yellow bands of GaN. Photoconductivity with below-band-gap excitation varies orders of magnitude with the wire diameter, similarly to that observed for near-band-edge excitation. Moreover, yellow-band-related signal shows a superlinear behavior with respect to the band-edge signal, offering new information for the modeling of the carrier recombination mechanism along the nanowires. The photoconductivity results agree well with a model which takes into account a uniform distribution of the localized states inside the wire and their direct recombination with the electrons in the conduction band.

KEYWORDS: nanowires · gallium nitride · spectral photoconductivity · yellow band

Semiconductor nanowires (NWs), in particular those based on wide-band-gap materials, have recently attracted great interest as they are very promising for a variety of applications such as optoelectronic, high-power, and high-operation-temperature devices, which could definitely change the scene of future technology.

The high surface-to-volume ratio of semiconductor NWs can dramatically alter the fundamental properties with respect to the corresponding bulk samples. Size can be therefore considered a key parameter, controlling the material properties as well as subsequent performance of the device.

Even though sophisticated NW device structures have already been demonstrated based on group III nitrides,[1−4] many fundamental questions regarding the effect of the large surface with respect to the bulk and size-dependent transport phenomena remain open to a large extent. In this context, previous investigations on GaN nanowires[5,6] revealed the effect of surface Fermi-level pinning and its interplay with the nanowire dimensions on the recombination behavior of photogenerated carriers. Particular emphasis has been given to the investigation of effects due to space charge layers in order to use them as design parameters for device performance.

Device optimization and engineering can be achieved only with a profound knowledge of the role of defects as well as their spatial distribution, their behavior, and their formation conditions. Indeed, many effects observed in bulk GaN can be partially ascribed to specific defects whose electronic levels lie within the large forbidden gap.[7−9] Deep levels, defined as defect-related energy levels located near the center of the band gap, may act as trapping or recombination centers for the free carriers, and therefore they may affect the carrier dynamics. The electrical transport mechanisms as well as the optoelectronic and optical behavior of NW structures can be completely exploited only after taking into account the defect-related electronic levels present in the forbidden gap. Notwithstanding the large amount of specific studies in bulk GaN,[10] the nature and the properties of the main defects are still under debate, especially with respect to GaN NWs. The aim of the present study is therefore a detailed investigation of the electrical and optoelectronic behavior of GaN NWs and its modeling in correlation with the deep levels detected.

All investigations reported here have been carried out on a set of more than 20 nanowires with diameters ranging between 50 and 500 nm.

RESULTS AND DISCUSSION

Conductivity Measurements. GaN nanowires analyzed in this work were grown by molecular beam epitaxy (MBE) on a Si(111)

*Address correspondence to laura.polenta@unibo.it.

Received for review November 26, 2007 and accepted January 17, 2008.

Published online February 7, 2008.
10.1021/nn700386w CCC: $40.75

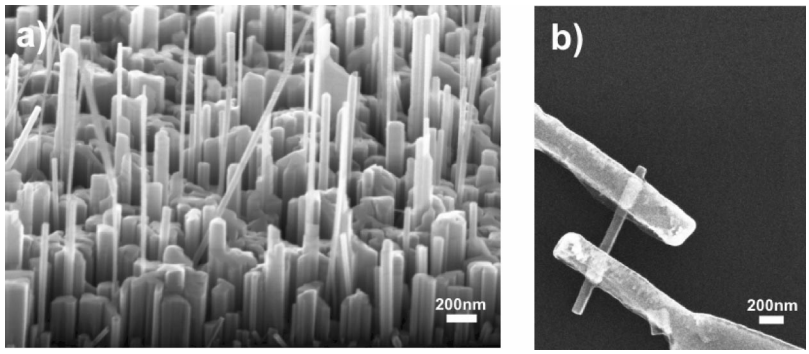

Figure 1. (a) SEM lateral side view of GaN nanowires as-grown. (b) SEM top view of a single nanowire device fabricated on a Si/SiO_2 host substrate, with Ti/Au contact electrodes. Nanowire diameter, 90 nm.

substrate.[11,12] The as-grown sample showed a wide distribution of hexagonal wires with diameters *d* ranging from 20 to 500 nm, and lengths from 0.3 to 2 μm, as shown in Figure 1a.

Figure 1b shows the secondary electron microscope image of a typical nanowire belonging to the set of the analyzed samples. Current–voltage characterization, carried out with and without ultraviolet (UV) illumination, shows a strong size dependence: dark conductivity σ, proportional to the free carrier density, is shown to increase exponentially with the diameter up to about 100–150 nm and approximately saturates for larger whiskers, as reported in Figure 2. A similar curve is obtained for UV photoconductivity.[5] Thereby, the electrical transport of carriers can be externally tuned just by making use of the nanowires' size.

Concerning the physical mechanism invoked for size-dependent conductivity, it has been proposed that the band bending, due to the Fermi-level pinning at the surface, creates depletion layers with an extension on the order of 50–100 nm, depending on doping concentration, and hence inhibits free carrier transport in thinner nanowires, which consequently behave as insulators. With increasing thickness, a thin conductive channel in the core of the nanowire may allow for conduction.[5] In addition, this space-charge layer model helps to explain the diameter dependence of the photocurrent obtained by above-band-gap illumination.

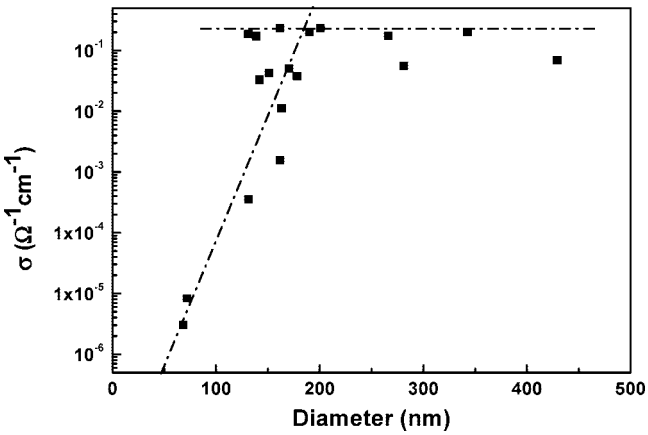

Figure 2. Dark conductivity as a function of wire diameter. The lines are guides for the eyes.

Persistent Photoconductivity *vs* Thickness. Complementary to the observation of the size dependence of dark conductivity, both photoconductivity and persistent photoconductivity effects are enhanced when increasing the nanowires' size, allowing a critical diameter, of approximately 80–100 nm, to be identified.[5] In the present paper, we were able to measure nanowires with a diameter down to 50 nm, while below this size the photocurrent drops under the measurement limit.

Persistent photoconductivity (PPC) is observed when the signal, after the removal of the UV light excitation, exhibits a noticeable delay before coming back to the dark value: the light-induced change in the free carrier concentration may also persist after switching off the optical excitation for minutes or hours.[13] PPC is a typical feature of GaN: it has been explained by a distribution of capture barriers with a mean capture barrier height of 0.2 eV,[9] due to the presence of bistable defects[14] or multiple charge-state defects related to nitrogen antisites and/or gallium vacancies.[15,16]

In GaN nanowires, the recovery to initial conditions is quasi-instantaneous for thin wires (with a donor concentration of 6.25×10^{17} cm^{-3} and diameter up to 80 nm) and becomes slower with increasing wire diameter.[5]

The analysis of the photoconductivity Δ*I* as a function of time *t* follows the stretched exponential model, commonly used for materials characterized by a nonexponential nature of the photoconductivity decay.[17] According to this model, the photoconductivity decay is described by the equation

$$\Delta I = \Delta I_{0d} \exp(-t/\tau)^{\beta} \quad (1)$$

where $\Delta I = I(t) - I(\mathrm{d})$ and $\Delta I_{0d} = I(t{=}0) - I(\mathrm{d})$, $I(t)$ being the current value at time *t* after the light is turned off, $I(d)$ the current measured keeping the sample in dark, and $I(t{=}0)$ the current after excitation. β is the stretching exponential, and τ is the decay time. In Figure 3, the photoconductivity relaxation diagrams for two nanowires of diameter 90 and 500 nm, respectively, are shown. The stretching exponential β is on the order of 0.11–0.18, while the values of τ range from 7 s in wires with diameter of about 90–100 nm, up to 20 s for wires as thick as 500 nm. Wires with diameter smaller than 80 nm do not show any photopersistent effect.

Although the space-charge layer effects[5] have been invoked to explain the diameter-related PPC behavior, defects can also contribute to the long time relaxation of photocurrent in thick samples. It is therefore neces-

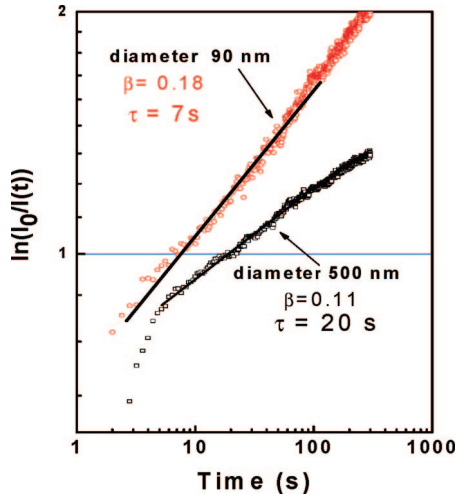

Figure 3. Current transient after 1 min of UV illumination (15 W/cm^2), acquired at a bias voltage of 2 V.

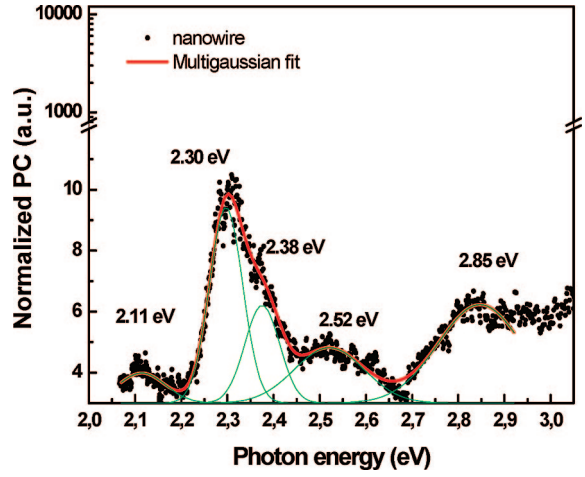

Figure 4. Spectral photoconductivity measurements in the visible range and relevant Gaussian deconvolution (green and red curves). Nanowire diameter, 90 nm.

sary to study possible correlations between PPC and the defect density as well as the role played by the recombination mechanism of bulk-located defects. Photopersistence effects in gallium nitride have often been correlated to the main defect-related band, known as the yellow band, and located about 2.2–2.3 eV below the conduction band.[7,8] Hence, it is appropriate to analyze the relationship between PPC and the NWs defects density as well as the role of defects in the recombination mechanisms.

Spectral Photoconductivity *vs* Thickness. Spectral photoconductivity (SPC) is a very efficient tool to investigate defect states responsible for optically induced transitions of carriers from defect-related bands to the conduction or valence bands in wide-band-gap materials.[15,18–20]

In the present set of NWs, in particular, SPC has been already revealed as a useful tool to evidence the presence of the Franz−Keldysh effect[6] and to detect interface-related defects.[19] Figure 4 shows the photoconductivity spectrum measured for the nanowire of Figure 1b, which has a diameter of about 90 nm and gives the highest signal-to-noise ratio among all samples.

The multi-gaussian fitting allows for analyzing the different transitions detected in detail. The double structure of the yellow band (YB) is clearly evident. The highest contribution, centered at 2.30 eV, corresponds to the yellow band zero phonon line ($h\nu_{YB}$) transition, while the shoulder peak at 2.38 eV is likely due to the longitudinal optical phonon replica ($h\nu_{YB} + \hbar\omega_{LO}$), where $\hbar\omega_{LO} = 92$ meV.[21,22] As a matter of fact, the strong phonon–electron coupling of deep levels in GaN has been reported.[10] Concerning the nature of this band, the scientific community is devoting major efforts toward definitely identifying its atomic structure, spatial distribution, and related transitions as well as properties of surface or bulk-related states,[23–25] since all these items are still under debate.

The blue band (BB), located at about 2.85 eV, is the second highest contribution, and its presence in undoped and unintentionally doped MBE-grown GaN compact layers has been suggested to be related to surface states.[26]

The green band (GB), located at 2.52 eV, is clearly distinguished in photoconductivity spectra, while its detection by luminescence is sometimes difficult.[10] In nanowires it has already been studied in terms of its relationship with the interface region.[19] Its contribution in non-nanometric samples is often comparable to that of the yellow band, while in nanowires it is reduced. We already suggested that, due to the bulk character of the green band, the high surface-to-volume ratio would be responsible for this low signal.[19]

What is important to focus on, however, is the behavior of such defect-related transitions in NWs and their evolution with sample size. Since blue and yellow bands are often invoked as being responsible for the PPC effects, we carried out spectral photoconductivity measurements on the set of samples with diameters ranging from 50 to 500 nm. In order to evidence the origin of the difference in electric transport, we need to compare the contributions of defective bands in differently sized nanowires.

The analysis procedure requires photoconductivity recording for each nanowire and subsequent normalization to the photon flux. As already observed, however, conductivity and photoresponse are different from wire to wire. It is therefore necessary to establish a method of comparison, as widely adopted in luminescence experiments: after the normalization to the photon flux, the signal is normalized to the peak intensity value at the band-gap energy. The ratio between defective band and band-gap signal is thus an estimation of the weight of a specific defect.

Figure 5 shows the photocurrent spectra obtained in wires of different diameters, from 50 to 350 nm, chosen in the sample set as representative of the general behavior. An interesting trend was observed concerning the presence of deep-level-related bands and their

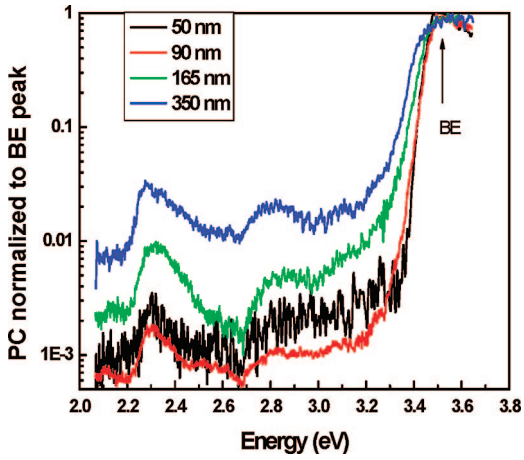

Figure 5. SPC spectra of four nanowires with different diameters. The photoconductivity signal is normalized to the band-edge peak intensity.

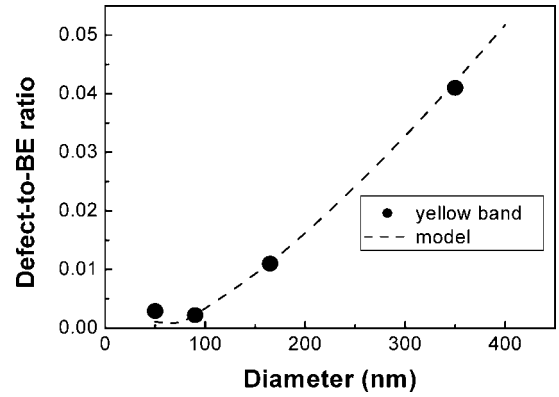

Figure 6. Ratio of the yellow band to band-edge contribution as a function of wire diameter. The dotted line corresponds to the theoretical fit.

contribution to the photocurrent spectra as a function of the nanowire size. Apart from the band tail occurring for energies just below the band-to-band transition, all spectra show similar features, in which yellow- and blue-band-related transitions dominate. Concerning the green band, located at 2.52 eV, its signal is better revealed in some wires, as represented in the spectrum shown in Figure 4. We recently demonstrated[19] the strong localization at the interface of the green-band-related defects, enhanced in the NW bottom section. The detection of such a band is therefore strictly related to the electrode position, *i.e.*, if the contact does include the interface region. Moreover, since the yellow band defects are homogeneously distributed along the whole wire, their contribution partially covers the localized contribution of the green band.

In the following we focus on the analysis of the blue- and yellow-band-related singals referring to the whole set of nanowires: (i) in thin wires (from 50 to 100 nm thick), the percent ratio between the yellow band and band edge, YB/BE, ranges from 0.2% to 0.4% and the percent ratio between blue band and band edge, BB/BE, from 0.1% to 0.2%; (ii) in thick wires (from 150 nm to 500 nm thick), YB/BE ranges from 2% to 4%, while BB/BE ranges from 0.5% to 2%.

It is worth noting that, with respect to the band-edge PC signal, both yellow and blue band intensities decrease by more than 1 order of magnitude when the diameter decreases below 100 nm.

To explain the observed increase of defect-induced SPC signal, a model is proposed in the following.

Modeling Results. To understand SPC behaviors, we have to consider different carrier recombination mechanisms subsequent to above-band-gap and sub-band-gap illumination. The physical mechanism that accounts for band-to-band transition by band-edge or above-band-gap illumination, explaining both photoconductivity and persistent photoconductivity behavior, is schematically shown in Figure 7a. The Fermi-level pinning at the surface of the GaN nanowire creates upward band bending and a surface depletion. Wires with diameter smaller than the depletion layer are expected to be completely depleted, and those with larger diameters may have a conducting channel.[5] This is the reason for the very strong dependence of the dark conductivity on the wire diameter in Figure 2. In addition, a hindered surface recombination due to the spatial separation of the carriers because of the band bending elucidates the persistent photocurrent for wires with diameters larger than the depletion layer. Further shrinking of the dimensions, however, causes less band curvature and therefore a reduction of the barrier for surface electron–hole pair recombination, which is thus enhanced.

The dependence of the photocurrent on wire diameter d can be evaluated considering generation and recombination of the photogenerated carriers. The generation rate at band-edge illumination is proportional to the probed volume, *i.e.*, proportional to the square of the wire diameter d. The photogenerated electrons move to the NW lateral surface to recombine with the photogenerated holes that, due to depletion layer field, reside already at the surface. Therefore, the recombina-

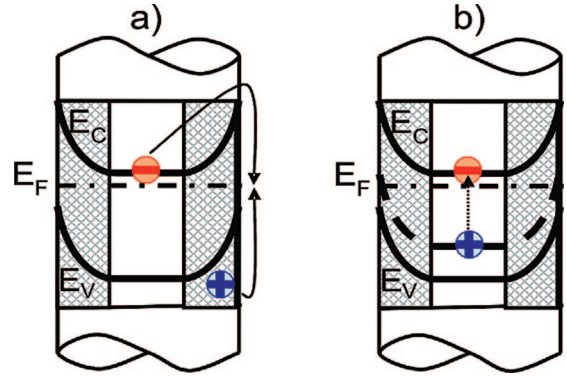

Figure 7. Energy band schema for GaN nanowires. The relative energetic locations of the trap E_C, E_V, and E_F are not to scale. (a) The detail on the right shows the surface recombination mechanism of the photoexcited carriers. (b) Direct recombination of a hole localized in the bulk, trapped at a yellow- or blue-band-related defect, with a free electron in the wire core.

tion rate S_r is proportional to the surface, *i.e.*, proportional to the diameter, and it is proportional to the total amount N of photogenerated carriers. For steady-state conditions, the generation rate G and recombination rate S_r of the photogenerated carriers are in equilibrium. Considering the relations $G = S_r$, $G \propto d^2$, and $S_r \propto dN$, we obtain $N \propto d$.

A more elaborate approach gives the following dependence of the photocurrent on d:

$$PC_{BE} \sim d(G/4n_0S_r) \exp(eV_0/kT) \quad (2)$$

where PC_{BE} is the photocurrent at band-edge illumination, n_0 the total carrier density in the wire center, and V_0 the surface potential relative to the center.

For sub-band-gap illumination, due to the fact that holes are localized and cannot drift to the wire surface, the recombination process is different than that for band−band processes. Only the photogenerated electrons can drift toward the wire center and must come back to the generated localized position to recombine with the localized holes.

To model the recombination of holes trapped at the acceptor-like defects responsible for yellow and blue bands at sub-band-gap illumination, we have assumed a uniform distribution of defects in the NW and consider the nanowire as containing two regions: the region in the center of the NW and the region close to the surface. In the latter region, due to the surface potential barrier and reduced probability for electrons to come back to the generated localized position, the recombination time for YB might be so large for a low defect density that the generated signal does not respond quickly to the PC chopped light. The localized states become almost empty, and generation is reduced. Thus, this region does not contribute to the alternating current signal. Therefore, only the core where the generation−recombination can follow the chopped light excitation contributes to the YB-PC signal. The carriers localized at the deep traps in the core are excited into the conduction band. The recombination between a hole localized in the core, trapped at a yellow- or blue-band-related defect, and a free electron is schematically shown in Figure 7b. Photoconductivity would be proportional to the volume of the core.[27]

Neglecting the difference between core and wire diameter, the photocurrent is almost proportional to the square of the diameter:

$$PC_{YB} \sim d^2 \quad (3)$$

As a consequence, the ratio of the photocurrents due to sub-band-gap and BE illumination (PC_{YB}/PC_{BE}) is proportional to the diameter. For a better fit of the experimental data, a bimolecular recombination term (a recombination path of direct electron–hole recombination) was included in the recombination formula of the BE photocurrent, and nanowires for which the surface recombination of the BE effect has a dominant contribution were considered. The fitting curve for YB-to-BE ratio is shown in Figure 6 (dotted line) up to a diameter of 400 nm. As already mentioned, noise- or geometry-related conditions affect the blue and green band signals; we therefore treat in detail only the mechanisms concerning the yellow band.

Due to the low density of the carrier in the conduction band within the surface depletion region (photoexcited electrons are separated from the original localized states by the internal electric field), the photoelectrons generated within this region by sub-band-gap illumination have a long recombination time and cannot respond to the chopped light excitation (3–5 Hz in our experiments). The photoconductivity produced within the depletion region contributes to a sub-band-gap PPC signal; therefore, only the effect restricted to a core region of the wire was taken into account in our model (see Figure 7b). A potential value increase of 0.1 eV relative to the wire center was used to delimit the core-region-related alternating current contribution in the photocurrent signal, and a critical diameter of 80 nm for a complete depleted wire was considered.

The diameter dependence of the ratio of defect-related and band-edge photoconductivity is a consequence of different recombination mechanisms and does not imply a size dependence of the defect density in the nanowires. Accounting for the electric field in the wire due to the surface band bending, the generation−recombination processes for BE and defect-related PC were modeled, and the dependence of the defect-to-BE photoconductivity ratio was evaluated as a function of the wire diameter.

Furthermore, electrical and photoelectrical properties such as conductivity and persistent photoconductivity of nanowires are mainly controlled by phenomena related to the depletion region of the NWs and do not correlate to the defect density.

FINAL REMARKS

In conclusion, we reported on conductivity and photoconductivity measurements carried out on GaN nanowires of diameters ranging from 50 to 500 nm, strongly dependent on the nanowire size.

We observed deep-level contributions in sub-band-gap photoconductivity as for compact layers: blue, green, and yellow bands. Under constant measurement conditions, the photoconductivity increases by many orders of magnitude with NW diameter. A model is proposed concerning the mechanism of carrier recombination for defect-related transitions, which, in contrast to band-to-band recombination, occurs directly between the free electrons in the wire core and the holes localized in the bulk and trapped at the yellow or blue bands.

EXPERIMENTAL METHODS

Material Synthesis and Preparation. GaN nanowires were grown by radio frequency plasma-assisted MBE on Si(111) substrates. N-rich conditions give rise to the wire structure.[10] The wires' density and diameter, ranging between 20 and 500 nm, can be controlled by monitoring the III/V ratio.

To carry out electrical conduction experiments, the nanowires were released from the native silicon substrate by exposure to an ultrasonic bath and deposited on a Si(100) host substrate covered with an insulation layer of SiO_2 (300 nm). Ohmic contacts of Ti/Au are patterned by electron beam lithography.[5]

Current–Voltage Measurements. The current–voltage as well as the time-dependent characteristics were studied on individually contacted wires by an HP4145B semiconductor parameter analyzer. UV illumination was provided by a mercury−xenon arc lamp whose light was directed to the device *via* a quartz fiber. The illumination power was approximately 15 W/cm^2.

Photoconductivity Measurements. A direct current voltage is supplied in order to keep a constant electric field driving the carriers through the electrodes and maintaining similar conditions of operation for all measurements.

A Xe lamp light source was used, entering a monochromator: from the output slit, the monochromatic beam is focused onto the sample, and hits the GaN surface with a chopper frequency of 3–5 Hz.

The photon flux ranges between 10^{13} and 10^{15} photons/cm$^2 \cdot$ s, depending on the wavelength. The photocurrent signal was collected by a lock-in amplifier. While the spectral range of wavelengths between 330 and 650 nm is covered, the variation of current signal due to the release of photogenerated carriers from deep traps evidences deep center-to-band transitions. Depending on the excitation wavelength, the carriers can gain enough energy to jump from a deep level to their respective bands, respectively from valence to conduction bands. Since the photocurrent is an image of the electrical conductivity, all transitions in the valence or conduction bands are observed, independent of their radiative or nonradiative character.

Photocurrent spectra have been subsequently normalized to the photon flux in order to quantitatively define the amplitude of the bands with respect to the band-gap-related transition.

The energy resolution is on the order of 0.01 eV in the range of the main defect bands (from 2.0 to 3.0 eV).

Acknowledgment. The authors thank K. H. Deussen for technical support. This research was carried out in the framework of the VIGONI program (www.crui.it) funded by MIUR (Ministero Istruzione Università e Ricerca) and DAAD (Deutscher Akademischer Austauschdienst).

REFERENCES AND NOTES

1. Zhong, Z.; Qian, F.; Wang, D.; Lieber, C. Synthesis of p-Type Gallium Nitride Nanowires for Electronic and Photonic Nanodevices. *Nano Lett.* **2003**, *3*, 343–346.
2. Qian, F.; Li, Y.; Gradecak, S.; Wang, D.; Barrelet, C.; Lieber, C. Gallium Nitride-Based Nanowire Radial Heterostructures for Nanophotonics. *Nano Lett.* **2004**, *4*, 1975–1979.
3. Hayden, O.; Agarwal, R.; Lieber, C. Nanoscale Avalanche Photodiodes for Highly Sensitive and Spatially Resolved Photon Detection. *Nat. Mater.* **2006**, *5*, 352–356.
4. Johnson, J. C.; Choi, H.-J.; Knutsen, K. P.; Schaller, R. D.; Yang, P.; Saykally, R. J. Single Gallium Nitride Nanowire Lasers. *Nat. Mater.* **2002**, *1*, 106–110.
5. Calarco, R.; Marso, M.; Richter, T.; Meijers, A. I.; Hart, A. v. d.; Stoica, T.; Lüth, H. Size-Dependent Photoconductivity in MBE-Grown GaN-Nanowires. *Nano Lett.* **2005**, *5*, 981–984.
6. Cavallini, A.; Polenta, L.; Rossi, M.; Stoica, T.; Calarco, R.; Meijers, R. J.; Richter, T.; Lüth, H. Franz-Keldysh Effect in GaN Nanowires. *Nano Lett.* **2007**, *7*, 2166–2170.
7. Reddy, C. V.; Balakrishnan, K.; Okomura, H.; Yoshida, S. The Origin of Persistent Photoconductivity and its Relationship with Yellow Luminescence in Molecular Beam Epitaxy Grown Undoped GaN. *Appl. Phys. Lett.* **1998**, *73*, 244–246.
8. Chen, H. M.; Chen, Y. F.; Lee, M. C.; Feng, M. S. Persistent Photoconductivity in n-type GaN. *J. Appl. Phys.* **1997**, *82*, 899–901.
9. Hirsch, M. T.; Wolk, J. A.; Walukiewicz, W.; Haller, E. E. Persistent Photoconductivity in n-type GaN. *Appl. Phys. Lett.* **1997**, *71*, 1098–1100.
10. Reschikov, M. A.; Morkoç, H. Luminescence Properties of Defects in GaN. *J. Appl. Phys.* **2005**, *97*, 061301.
11. Calarco, R.; Meijers, R. J.; Debnath, R. K.; Stoica, T.; Sutter, E.; Luth, H. Nucleation and Growth of GaN Nanowires on Si(111) Performed by Molecular Beam Epitaxy. *Nano Lett.* **2007**, *7*, 2248–2251.
12. Meijers, R.; Richter, T.; Calarco, R.; Stoica, T.; Bochem, H.-P.; Marso, M.; Lüth, H. GaN-Nanowhiskers: MBE-growth Conditions and Optical Properties. *J. Cryst. Growth* **2006**, *289*, 381–386.
13. Queisser, H. J.; Theodorou, T. E. Decay Kinetics of Persistent Photoconductivity in Semiconductors. *Phys. Rev. B* **1986**, *33*, 4027–4033.
14. Park, C. H.; Chadi, D. J. Stability of Deep Donor and Acceptor Centers in GaN, AlN, and BN. *Phys. Rev. B* **1997**, *55*, 12995–13001.
15. Qiu, C. H.; Pankove, J. I. Deep Levels and Persistent Photoconductivity in GaN Thin Films. *Appl. Phys. Lett.* **1997**, *70*, 1983–1985.
16. Lin, Y.; Yang, H. C.; Chen, Y. F. Optical Quenching of the Photoconductivity in n-type GaN. *J. Appl. Phys.* **2000**, *87*, 3404–3408.
17. Qiu, C. H.; Hoggatt, C.; Melton, W.; Leksono, M. W.; Pankove, J. I. Study of Defect States in GaN Films by Photoconductivity Measurement. *Appl. Phys. Lett.* **1995**, *66*, 2712–2714.
18. Bube, R. H. *Photoconductivity of Solids*; John Wiley and Sons, Inc.: New York, 1960.
19. Cavallini, A.; Polenta, L.; Rossi, M.; Richter, T.; Marso, M.; Meijers, R.; Calarco, R.; Lüth, H. Defect Distribution along Single GaN Nanowhiskers. *Nano Lett.* **2006**, *6*, 1548–1551.
20. Polenta, L.; Castaldini, A.; Cavallini, A. Defect Characterization in GaN: Possible Influence of Dislocations in the Yellow-band features. *J. Appl. Phys.* **2007**, *102*, 063702.
21. Castaldini, A.; Cavallini, A.; Polenta, L. Yellow and Green Bands in GaN by Resolved Spectral Photoconductivity. *Appl. Phys. Lett.* **2005**, *87*, 122105.
22. Jenny, J.; Jones, R.; Van Nostrand, J. E.; Reynolds, D. C.; Look, D. C.; Jogai, B. Source of the Yellow Luminescence Band in GaN Grown by Gas-Source-MBE and the Green Luminescence Band in Single Crystal ZnO. *Solid State Commun.* **1998**, *106*, 701–704.
23. Hsu, J. W. P.; Schrey, F. F.; Ng, H. M. Spatial Distribution of Yellow Luminescence Related Deep Levels in GaN. *Appl. Phys. Lett.* **2003**, *83*, 4172–4174.
24. Reschikov; M. A.; Morkoç, H.; Park, S. S.; Lee, K. Y. Two Charge States of Dominant Acceptor in Unintentionally Doped GaN: Evidence from Photoluminescence Study. *Appl. Phys. Lett.* **2002**, *81*, 4970–4972.
25. Shalish, I.; Kronik, L.; Segal, G.; Rosenwaks, Y.; Shapira, Y.; Tisch, U.; Salzman, J. Yellow Luminescence and Related Deep Levels in Unintentionally doped GaN films. *Phys. Rev. B* **1999**, *59*, 9748–9751.
26. Reschikov; M. A.; Visconti, P.; Morkoç, H. Blue Photoluminescence Activated by Surface States in GaN grown by Molecular Beam Epitaxy. *Appl. Phys. Lett.* **2001**, *78*, 177–179.
27. Chen, I. Effects of Bimolecular Recombination on Photocurrent and Photoinduced Discharge. *J. Appl. Phys.* **1978**, *49*, 1162–1172.